Published in final edited form as:

Cell Rep. 2024 April 23; 43(4): 113991. doi:10.1016/j.celrep.2024.113991.

Tactile processing in mouse cortex depends on action context

Eric A. Finkel[1], **Yi-Ting Chang**[1,2], **Rajan Dasgupta**[1,2], **Emily E. Lubin**[1], **Duo Xu**[1], **Genki Minamisawa**[1], **Anna J. Chang**[1], **Jeremiah Y. Cohen**[1], **Daniel H. O'Connor**[1,3,*]

[1]Solomon H. Snyder Department of Neuroscience, Krieger Mind/Brain Institute, Kavli Neuroscience Discovery Institute, Johns Hopkins University, Baltimore, MD 21218, USA

[2]These authors contributed equally

[3]Lead contact

SUMMARY

The brain receives constant tactile input, but only a subset guides ongoing behavior. Actions associated with tactile stimuli thus endow them with behavioral relevance. It remains unclear how the relevance of tactile stimuli affects processing in the somatosensory (S1) cortex. We developed a cross-modal selection task in which head-fixed mice switched between responding to tactile stimuli in the presence of visual distractors or to visual stimuli in the presence of tactile distractors using licking movements to the left or right side in different blocks of trials. S1 spiking encoded tactile stimuli, licking actions, and direction of licking in response to tactile but not visual stimuli. Bidirectional optogenetic manipulations showed that sensory-motor activity in S1 guided behavior when touch but not vision was relevant. Our results show that S1 activity and its impact on behavior depend on the actions associated with a tactile stimulus.

Graphical abstract

*Correspondence: dan.oconnor@jhmi.edu.

AUTHOR CONTRIBUTIONS

Conceptualization, E.A.F. and D.H.O.; investigation, E.A.F., Y.-T.C., R.D., E.E.L., and G.M.; methodology, E.A.F., Y.-T.C., R.D., D.X., G.M., and A.J.C.; formal analysis, E.A.F., Y.-T.C., R.D., and D.X.; writing – original draft, E.A.F., Y.-T.C., R.D., D.X., and D.H.O.; writing – review & editing, E.A.F., Y.-T.C., R.D., D.X., and J.Y.C.; funding acquisition, D.H.O. and J.Y.C.; resources, D.H.O. and J.Y.C.; supervision, D.H.O.

SUPPLEMENTAL INFORMATION

Supplemental information can be found online at https://doi.org/10.1016/j.elrep.2024.113991.

DECLARATION OF INTERESTS

The authors declare no competing interests.

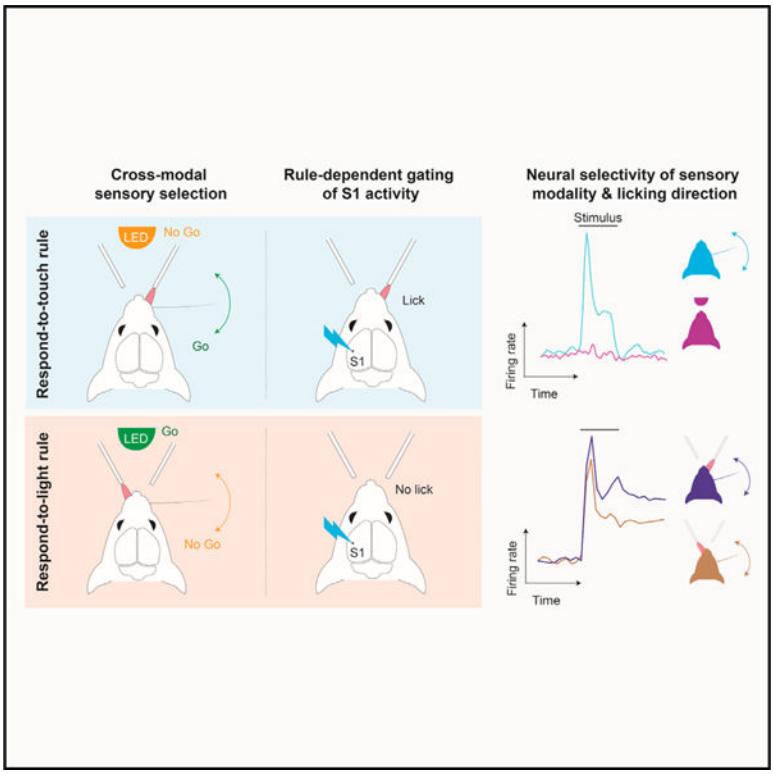

In brief

Finkel et al. use a cross-modal detection task for mice with single-unit recordings and optogenetic perturbations to investigate the relationship between the early cortical processing of a tactile stimulus and its behavioral relevance. S1 activity and its impact on behavior depend on the relevance of tactile stimuli to specific actions.

INTRODUCTION

Tactile and other sensory stimuli typically occur in the context of an ongoing or intended action. In many real-world scenarios, sensory input triggers actions in a context-specific manner.[1] A driver steps on the brake upon seeing a stop sign, but a passenger ignores the same stop sign. The relevance of this sensory input—the stop sign—is determined by the action it requires. The actions and relevance associated with a tactile stimulus must be reflected in sensory-motor brain activity.

A tight relationship between sensation, stimulus relevance, and movement is captured by the ‘‘premotor’’ theory of attention, which posits that attentional selection of relevant stimuli is mediated by activity of motor-related brain circuits.[2,3] In this framework, even covert shifts of attention are driven by activation of motor circuitry at levels subthreshold for evoking movements but which enhance processing for the selected or attended stimulus.[4–8] Motor signals can thus play a direct role in sensory processing.

We investigated whether and how the relevance of a stimulus, and the actions associated with it, modulate tactile processing in the somatosensory cortex. We designed a cross-modal selection task for head-fixed mice that required different actions in response to a tactile or visual stimulus, depending on context. In different blocks of trials, mice responded either to a tactile stimulus while ignoring visual distractors or to a visual stimulus while ignoring tactile distractors. Thus, the behaviorally relevant sensory modality alternated between touch and vision. Detection of each stimulus modality required a distinct licking-based action. Our results demonstrate that tactile processing depends on the behavioral relevance of a stimulus and on the specific actions it requires.

RESULTS

A cross-modal selection task for head-fixed mice

We designed a cross-modal sensory selection task for head-fixed mice[9] in which mice learned to switch between (1) detecting tactile stimuli while ignoring visual stimuli (‘‘respond-to-touch’’ block) and (2) detecting visual stimuli while ignoring tactile stimuli (‘‘respond-to-light’’ block). Mice switched between respond-to-touch and respond-to-light blocks multiple times per session (Figure 1A; 3–5 blocks per session, each containing ~80 trials). Tactile stimuli comprised a brief single-whisker deflection on the right side of the face. Visual stimuli comprised a brief light flash emitted from the tip of an optic fiber placed in front of the mouse. Mice were trained to respond to a whisker stimulus occurring in a respond-to-touch block by licking to a spout placed to the right of the mouse’s midline, and to withhold licking in response to this stimulus during respond-to-light blocks. Similarly, mice had to respond to a visual stimulus in respond-to-light blocks by licking to a spout placed to the left of the mouse and to withhold licking in response to visual stimuli during respond-to-touch blocks (Figure 1A). Correct responses to both tactile and visual stimuli (‘‘hits’’) were rewarded with a drop of water (Figure 1A). Correctly withheld responses (‘‘correct rejections’’) were unrewarded. Failures to respond to tactile stimuli in respond-to-touch blocks or visual stimuli in respond-to-light blocks were scored as errors (‘‘misses’’) but not punished. Responses to the inappropriate stimulus type, or at the incorrect spout, were scored as error trials (‘‘false alarms’’) and neither rewarded nor punished. Blocks were distinguished by reward availability but not overtly cued. Mice switched strategies via trial-and-error on approximately one-third of trials. On the remaining trials, mice failed to switch within ~10 trials, and a drop of water was delivered to the rewarded spout to signal the block change.

Mice learned the task over 2–4 weeks (Figures 1B–1D). After training, detection accuracy (percentage of trials correct) was similar for respond-to-touch and respond-to-light blocks (Figures 1E and 1F; respond-to-touch: 72.8% ± 0.5% correct, mean ± SEM; respond-to-light: 75.1% ± 1.0% correct; $p = 0.093$, paired samples t test, $n = 11$ mice). Reaction times were slightly shorter for tactile stimuli (Figure 1G; tactile vs. visual for 150-ms stimuli: 397 ± 145 vs. 521 ± 163 ms, median ± interquartile range, Tukey’s HSD test, $p = 0.001$, $n = 155$ sessions; for 50-ms stimuli: 401 ± 155 ms vs. 523 ± 155 ms, $p = 0.001$, $n = 122$ sessions). Mice therefore flexibly switched between detecting either tactile or visual stimuli while rejecting distractors of the other type.

Relevance-dependent sensory and motor activity in S1

To examine how the relevance of tactile stimuli and their associated actions affect cortical processing, we obtained single-unit recordings from left S1 (contralateral to the stimulated whisker; Figures 2A and 2B). We compared responses to tactile stimuli within a respond-to-touch block, where tactile stimuli required a response and were thus relevant to behavior, with responses to tactile stimuli within a respond-to-light block, which required no response and could thus be ignored (Figure 2C). To help ensure that analysis included only tactile stimuli that the mouse correctly treated as relevant or ignorable, we restricted analysis to correct trials. Beginning ~25 ms after stimulus onset, responses to the tactile stimulus were on average slightly larger when occurring in a respond-to-touch block (Figures 2C and S1; tactile hits vs. tactile correct rejections [CRs]: 12.61 ± 0.37 Hz vs. 11.62 ± 0.33 Hz in 25-ms bin starting at 25 ms after stimulus onset, mean ± SEM; $n = 1{,}539$ neurons; $p = 7.4 \times 10^{-4}$, two-sided Wilcoxon signed-rank test). Relevant tactile stimuli thus evoked larger S1 responses. Because the relevance of a stimulus in our task was defined by whether it required licking, these larger responses may reflect both sensory and motor-related activity.

During respond-to-touch blocks, neural responses to the whisker stimulus occurred on both hits and misses (mean Z score in a window 0–150 ms after stimulus onset: tactile hits 0.88 ± 0.09, mean ± SEM; $p < 0.0001$, permutation test; tactile misses 0.40 ± 0.06, $p < 0.0001$; $n = 1{,}539$ neurons). However, activity on tactile hits was on average larger than on tactile misses (Figures 2B–2E; difference in mean Z scores between tactile hits and tactile misses in a window 0–500 ms after stimulus onset: 0.98 ± 0.08, mean ± SEM; $p < 0.0001$, permutation test; $n = 1{,}539$ neurons). In addition, activity on tactile hits but not tactile misses remained elevated until the reaction time or later (Figures 2B–2E; mean Z score in a window 150–500 ms after stimulus onset: tactile hits 1.31 ± 0.08, mean ± SEM; $p < 0.0001$, permutation test; tactile misses 0.12 ± 0.04, $p = 0.467$; $n = 1{,}539$ neurons). This is consistent with the observation of enhanced hit vs. miss responses in prior work using simple tactile detection tasks.[10–15] On tactile false alarms, mean activity also exceeded baseline prior to licks (Figures 2B–2E; false alarms: mean Z score in a window 0–500 ms after stimulus onset 0.5 ± 0.06, mean ± SEM; $p < 0.0001$, permutation test; $n = 1{,}539$ neurons).

On visual correct rejections in which visual stimuli were presented but mice successfully made no response, activity did not exceed baseline (Figures 2B–2E; visual CRs: mean Z score in a window 0–500 ms after stimulus onset, −0.04 ± 0.03, mean ± SEM; $p = 0.67$, permutation test; $n = 1{,}539$ neurons). During respond-to-light blocks, we also observed no obvious response to the visual stimuli on visual misses, in which mice made no response (Figures 2B–2E; visual misses: mean Z score in a window 0–150 ms after stimulus onset, −0.04 ± 0.04, mean ± SEM; $p = 0.65$, permutation test; $n = 1{,}539$ neurons). Responses to the tactile stimulus were evident in respond-to-light blocks (Figures 2B and 2D; tactile CRs: mean Z score in a window 0–150 ms after stimulus onset, 0.35 ± 0.06, mean ± SEM; $p < 0.0001$, permutation test; $n = 1{,}539$ neurons). On visual hits and false alarms but not misses, activity was elevated for hundreds of milliseconds prior to the lick (Figures 2B–2E).

Although S1 activity was strongly associated with licking, alignment of each neuron's activity to individual licks (the first to fourth licks in a bout) revealed few neurons (<10%) with activity that followed individual lick cycles (Figures S2A and S2C, bottom row).

Rather, most neurons showed activity that peaked well before the first lick and did not closely track subsequent licks (Figures S2B and S2C, top row).

Together, these results show that S1 activity reflected tactile but not visual responses, and motor activity was associated with licking responses.

Our task required mice to switch between two stimulus-response ‘‘rules.’’ S1 activity differed between block types (Figure 2), raising the possibility of modulation by a neural representation of the rule itself. Alternatively, S1 activity could comprise only the sensory and motor activity resulting from application of the rule. We reasoned that if the rule itself modulated S1 activity, we might observe changes in activity occurring around the time of block transitions that were not attributable to the sensory stimulus or the mouse’s response. To address this, we trained a separate group of mice ($n = 6$) on a version of our task modified to have more frequent block transitions. Mice were not immediately cued to the block transitions but could detect the rule change through trial and error over the first few trials. On the ninth trial, a drop of water was delivered to the rewarded port to signal the block transition to any mice that had failed to detect it.

Error trials indicative of the mouse applying the wrong rule, e.g., licking the right port in response to a tactile stimulus during a respond-to-light block, tended to occur during the first nine trials (Figures S3B and S3C). Most correct trials occurred later than the first nine trials (Figures S3A and S3E). This pattern indicates that mice typically switched rules at a point close to the ninth trial. We therefore grouped trials into those occurring either ‘‘early’’ ($<9^{th}$ trial) or ‘‘late’’ ($>9^{th}$ trial) following the block change (Figure S3), and by block type and the mouse’s response. We included only trials with a tactile stimulus. This grouping allowed comparison of neural responses occurring mostly before or mostly after the mouse’s rule change, having equated stimulus, action, and block type (Figure S3). Only ~1% of neurons showed a significant difference in mean response between early and late trials (2 of 177 from six mice; permutation tests on peristimulus spike time histograms (PSTHs),[16–18] Bonferroni corrected for multiple comparisons). S1 neurons were therefore unaffected by the rule switch per se, indicating that larger tactile responses in respond-to-touch blocks (Figure 2) reflected sensory and motor activity alone.

Trial-by-trial sensory and motor encoding in S1

We examined more closely how the activity of S1 neurons was related to the stimulus and licking response. S1 activity clearly depended on the stimulus condition (tactile or visual) and on the response of the mouse (lick or no lick; Figure 2). Our task design included both long-duration (150 ms) and short-duration (50 ms) tactile and visual stimuli. We therefore grouped trials into eight types (two stimulus modalities × two durations × two possible responses) and examined the mean spiking response for each type. As expected, long tactile stimuli evoked a more protracted evoked response over the first 150 ms after stimulus onset (Figures 3A and 3B), reflecting the tactile responsiveness of S1 neurons. Similarly expected, activity was identical for both long and short visual stimuli, reflecting the lack of visual responsiveness of S1 neurons in our task (Figures 3A and 3B).

We used ideal-observer analysis to quantify how well the single-trial activity of individual neurons could be used to discriminate the presence of the stimulus (‘‘stimulus probability’’ [SP]) or predict the mouse’s response (‘‘detect probability’’ [DP][19,20]). S1 neurons signaled the presence of tactile stimuli on a trial-by-trial basis (95% confidence interval [CI] for SP did not include 0.5), with long tactile stimuli producing a more prolonged elevation of SP (short vs. long tactile stimuli: 7 vs. 4 bins of 25 ms with SP different from 0.5 for neuron in Figure 3C). S1 neurons did not signal the presence of visual stimuli (Figure 3C). Individual S1 neurons could also predict the licking response of the mouse (95% CI for DP did not include 0.5; Figure 3D).

Individual neurons could predict the licking response for both tactile (right-side) and visual (left-side) licks (example indicated by green in Figures 3E–3I) or less commonly for only tactile licks (blue example) or only visual licks (red example). Most neurons predicted licking to both sides, with an overall slight bias to better predict licking responses for tactile stimuli (Figures 3F–3I). A neuron could predict licking without being able to signal the presence of a stimulus (Figure 3F). Most neurons that signaled stimulus presence or licking did so with increased firing rates (794 of 1,539 neurons), but some showed decreased rates (356 of 1,539 neurons; Figure 3G).

DP onsets occurred earlier for tactile trials (Figure 3J; two-sided Kolmogorov-Smirnov test, $p = 1\ 3\ 10^{-16}$, $n = 865$ neurons with DP onset in tactile trials, $n = 719$ neurons with DP onset in visual trials). This was not explained by reaction times (Figure S4). Thus, S1 neurons predicted licking for both tactile and visual stimuli, but earlier for tactile stimuli.

S1 neurons encode the direction of lick responses, but only for tactile stimuli

So far, direction of licking was confounded with stimulus modality: mice licked right for tactile stimuli but left for visual stimuli. To determine whether differences in licking-related activity following tactile vs. visual stimuli were due strictly to lick direction, we modified the task to include two new block types: one where mice licked to the left to tactile stimuli (but without visual distractors) and one where mice licked to the right to visual stimuli (without tactile distractors; ‘‘lick-direction-switch task’’; Figures 4A and S5). In each session, mice therefore licked either to the right or to the left in response to tactile stimuli (in different blocks) and licked either to the left or to the right in response to visual stimuli (in different blocks). We recorded from whisker S1 in these mice ($n = 3$).

Activity in correct trials from respond-right-to-touch/ignore-light blocks was greater than in correct trials from respond-left-to-touch blocks following tactile stimulus onset (Figures 4B and 4C; difference in mean Z scores between respond-right-to-touch/ignore-light and respond-left-to-touch trials: 0.14 ± 0.07, mean ± SEM; $p = 3.0\ 3\ 10^{-4}$, one-sided paired t test on first 150-ms bin; $n = 375$ neurons). In contrast, activity was similar for trials from respond-right-to-light and respond-left-to-light/ignore-touch blocks (Figures 4B and 4C). We used ideal-observer analysis to quantify how well individual neurons discriminated (1) the presence vs. absence of licking and (2) the lick direction. Neurons signaled licking in response to both visual and tactile stimuli (Figure 4D, green curves). For tactile but not visual stimuli, neurons also signaled lick direction for hundreds of milliseconds following stimulus onset (Figure 4D, blue curves, $p < 1 \times 10^{-3}$, one-sided one-sample t test on first

150-ms bin; $n = 375$ neurons). Thus, single neurons encoded lick direction for tactile but not visual stimuli.

The additional block types in the ‘‘lick-direction-switch’’ task (respond-left-to-touch and respond-right-to-light) had no distractors (Figure 4A). Greater activity in respond-right-to-touch/ignore-light blocks compared with respond-left-to-touch blocks (Figure 4C) might thus result from unequal difficulty. We compared mice trained in the normal cross-modal selection task (Figure 1A) with mice trained in the same task with opposite contingencies, such that tactile stimuli produced licking to the left and visual stimuli licking to the right (Figure S6). Mice trained in the normal task showed greater DP for tactile stimuli compared with mice trained to lick left to tactile stimuli ($p = 1 \times 10^{-2}$, two-sided t test; respond-right-to-touch, $n = 1{,}539$ neurons; respond-left-to-touch, $n = 549$ neurons; Figure S6). Thus, consistent with results from the ‘‘lick-direction-switch’’ task, activity was enhanced for contraversive licking to tactile stimuli.

Motor-related activity is not due to whisker input

Recent work has emphasized the role of movements, including those uncontrolled by the experimenter, in shaping brain activity.[21–26] Licking-related activity in S1 could potentially result from uncontrolled sensory input from whiskers. We obtained high-speed videos from a new set of mice ($n = 6$) to analyze whisker motion. We tracked positions of the stimulated whisker and a second (‘‘surrogate’’) whisker used to monitor whisking (Figure 5A; 4,377 videos across 14 sessions in total from six mice).

We assessed whether whisking during the pre-stimulus period differed between respond-to-touch and respond-to-light blocks, tactile trials with and without a lick response, and visual trials with and without a lick response. For each session, we used ideal-observer analysis to quantify how well the standard deviation of surrogate whisker angle over the pre-stimulus trial period could be used to discriminate between trial types. We found no significant discriminability (99.6% CI on the area under the receiver-operating characteristic [ROC] curve included 0.5; confidence level determined using Bonferroni correction for a 5% family-wise false-positive rate) for most sessions (12 of 14 sessions for the respond-to-touch vs. respond-to-light blocks comparison; 11 of 14 sessions for tactile lick vs. tactile no-lick trials; 11 of 14 sessions for visual lick vs. visual no-lick). Thus, pre-stimulus whisking does not reliably differ between block types or between trials in which the mouse did or did not lick in response to the stimulus.

While the whisker stimulator pipette was in a reproducible position on every trial, the mouse was free to move the follicle of the stimulated whisker. This would produce changes in the pre-stimulus angle of the stimulated whisker and potentially cause systematic differences in the amplitude of the whisker stimulus. However, 0 of 14 sessions showed a significant difference between tactile lick and tactile no-lick trials in the measured amplitude of the whisker stimulus (99.6% CI on area under the curve included 0; Bonferroni correction for a 5% family-wise false-positive rate). Differences in amplitude were not correlated with differences in pre-stimulus whisker angle (Figure S7;$r = -0.12$, $p = 0.72$). Thus, stimulus amplitude did not reliably differ between tactile lick and tactile no-lick trials.

We assessed how changes in whisker position following stimulus onset were associated with the occurrence and timing of licks. We calculated ‘‘whisker DP,’’ calculated identically to neural DP but using whisker angle. Whisker DP exceeded chance level at some point following stimulus onset, indicating that whisker position differed between trials with and without licks (Figure 5B). If licking-related activity in S1 arose because of sensory input from the whisker motions that accompanied the onset of licking, there should be a correlation between the onset times of whisker DP and behavioral reaction times. However, similar to neural DP (Figure S4), we did not find a consistent session-by-session relationship between whisker DP onset times and licking reaction times (tactile trials: r = 0.19, $p = 0.52$; visual trials: r = 0.02, $p = 0.96$; Figure 5C).

If licking-related activity arose entirely from whisker input, the earliest DP onset times should lag behind the onset times of whisker DP. We compared the distribution of the earliest neural DP onset occurring in each recording session against the distribution of whisker DP onsets. Because we did not record high-speed videos during our electrophysiology recording sessions, these distributions came from different groups of mice. The earliest neural DP onsets following tactile stimuli slightly preceded whisker DP onsets, indicating that neural DP could not entirely be explained by post-stimulus whisker motion (Figure 5D; earliest neural DP onsets: 100 ms ± [50 ms, 150 ms], median ± [25th, 50th percentiles]; $n = 126$ neurons; surrogate whisker DP onsets: 166 ms ± [51 ms, 226 ms]; $n = 14$ sessions; one-sided Kolmogorov-Smirnov test, $p = 0.032$).

Together, our high-speed video analyses show that differences in S1 activity that we attributed to stimulus relevance or licking cannot be parsimoniously explained by uncontrolled variability in whisker input.

S1 activity is gated based on the relevance of touch

To test whether S1 activity promotes detection in a manner dependent on the relevance of touch, we trained new Emx1-Cre;Ai32 mice in the cross-modal selection task. We included trials (20%) in both respond-to-touch and respond-to-light blocks in which S1 excitatory neurons were optogenetically excited in place of a sensory stimulus (Figure 6A). During respond-to-touch blocks, excitation increased lick rates to levels comparable to those of tactile stimulation (Figures 6B and 6C; 95% CI on difference includes 0, $n = 4$ mice). Excitation during respond-to-light blocks, in contrast, did not produce lick rates comparable to those of visual stimulation (Figures 6B and 6C; 95% CI does not include 0, $n = 4$ mice). Excitation of S1 therefore promoted lick responses specifically during respond-to-touch but not respond-to-light blocks.

In complementary experiments, we optogenetically inhibited S1 via excitation of GABAergic neurons[12,27] in PV-Cre;Ai32 mice (Figure 7). On ~30% of trials we inhibited S1 in a 1.5-s window beginning either simultaneously with, or delayed by 50 ms with respect to, the onset of the tactile or visual stimulus (Figure 7A). Thus, we inhibited either during a period ranging from stimulus onset to typical reaction times or beginning after the initial sensory response but capturing the later sensory-motor activity (see also Sachidhanandam et al.[12,28] and Resulaj et al.[12,28]). We also included ‘‘catch’’ trials (~20%), in which we

inhibited in the absence of tactile or visual stimuli, to confirm that mice did not treat the optogenetic excitation light as task-relevant visual stimuli.

S1 recordings during a subset of experiments showed that the majority of neurons were inhibited (Figures 7B and 7C), but a small number of presumably GABAergic neurons were strongly excited (Figure 7C, top of right heatmap). These recordings also showed that for neurons that could predict the presence of the stimulus on a trial-by-trial basis (those with 95% CI for SP that did not include 0.5 for two consecutive bins), delayed inhibition left intact the early tactile response whereas simultaneous inhibition did not (Figure 7D; sign tests on Δspike rate for time bins of [0 ms, 50 ms] and [50 ms, 100 ms] relative to stimulus onset, respectively; delayed inhibition: $p = 0.5$ and $p = 0.052$; simultaneous inhibition: $p = 0.052$ and $p = 0.013$; $n = 46$ neurons).

During respond-to-touch blocks, detection of tactile stimuli was reduced following simultaneous inhibition of S1 (Figures 7E and 7F; Δp(lick) = −0.42 ± [−0.51, −0.33], mean ± 95% CI). Inhibiting S1 at a 50-ms delay from tactile stimulus onset reduced detection, but less so than simultaneous inhibition (Figures 7E and 7F; delayed: Δp(lick) = −0.19 ± [−0.28, −0.09], mean ± 95% CI; simultaneous vs. delayed: −0.23 ± [−0.30, −0.16]). In contrast, S1 inhibition had a negligible impact on detection performance during respond-to-light blocks (Figures 7E and 7F; simultaneous: Δp(lick) = −0.08 ± [−0.14, −0.02], mean ± 95% CI; delayed: Δp(lick) = −0.02 ± [−0.08, 0.03]). There was no significant difference for simultaneous vs. delayed inhibition during respond-to-light-blocks (Δp(lick) = −0.06 ± [−0.14, 0.03], mean ± 95% CI). Thus, S1 inhibition severely impaired performance in respond-to-touch but not respond-to-light blocks.

In experiments with different mice, we directed light bilaterally to primary visual cortex (V1) instead of S1 and found impaired performance during respond-to-light but not respond-to-touch blocks (Figures 7G–7I; $n = 5$ mice, 41 sessions in total).

Together, results from S1 excitation and inhibition experiments indicate that performance depended on S1 activity when touch but not vision was relevant.

DISCUSSION

We developed a cross-modal selection task in which mice flexibly switched between responding to tactile stimuli while ignoring visual distractors or responding to visual stimuli while ignoring tactile distractors. Our task allowed the study of how actions associated with tactile stimuli, and thus their behavioral relevance, impact stimulus processing. We found a prominent role for motor signals in S1. S1 controls whisker retractions via projections to brainstem premotor nuclei[29–31] and may be fundamentally a sensory-motor structure. Although we used passive whisker stimulation to avoid complexities of active touch tasks, in which rodents move their whiskers to generate tactile input (e.g., von Heimendahl et al.,[32–36] Isett et al.,[32–36] Knutsen et al.,[32–36] Mehta et al.,[32–36] and O'Connor et al.[32–36]), our results highlight the sensory-motor nature of touch and reinforce findings on motor → sensory influences in rodent S1.[37–39]

Adding S1 activity promoted licking during respond-to-touch but not respond-to-light blocks. This indicates that S1 activity is readout for whisker detection task performance[12] specifically in contexts during which touch is behaviorally relevant. Prior work used optogenetic excitation of layer 4 neurons in specific whisker barrels that either corresponded to (the C2 barrel) or did not correspond to (the E3 barrel) the whisker mice used to solve an active tactile localization/detection task.[40] Stimulation of the C2 but not the E3 barrel ''fooled'' the mice into responding as though the whisker had actively touched an object, but only during epochs of active whisking. A context-specific readout of S1 activity based on its relevance to the task at hand may therefore be a common feature of different whisker-based tasks.

Inhibiting S1 activity degraded performance in respond-to-touch blocks but did so negligibly during respond-to-light blocks. This is consistent with work showing that S1 silencing disrupts tactile but not auditory detection when mice must detect randomly interleaved stimuli of either modality.[41] Optogenetic S1 silencing therefore does not cause non-specific deficits in detection task performance. By silencing throughout the full period of stimulus delivery, or only beginning 50 ms after stimulus onset (see Sachidhanandam et al.[12]), we found that even late activity impacted performance only when touch was relevant. This supports earlier work demonstrating an impact of late activity on tactile detection.[12] Behavioral impacts of silencing sensory cortex at different times relative to stimulus onset may depend on the specific demands of the task.[42] Accumulating evidence shows that transient optogenetic silencing of somatosensory cortex impairs performance on whisker-based detection and similar tasks.[10,12,15,27,40,41,43] Rodents can, however, learn to perform detection tasks without barrel cortex,[43,44] suggesting that circuits for relevant sensory-motor transformations are redundant and/or capable of flexible remapping.

Limitations of the study

Analysis of high-speed video during task performance led us to conclude that uncontrolled variability in whisker input does not explain our key findings. We analyzed multiple aspects of whisker motion, but other whisker mechanical signals that could not be extracted from our video might correlate with task-related S1 activity. Orofacial movements are highly correlated,[45,46] and it is plausible that uncontrolled input from other orofacial structures could show up as licking-related activity in whisker S1. ''Gold-standard'' evidence that uncontrolled tactile input does not explain our results will require new experiments in which high-speed video of whiskers and other orofacial structures are acquired simultaneously with S1 recordings during task performance.

We found that optogenetic excitation of S1 promoted licking during respond-to-touch but not respond-to-light blocks and interpret this result as evidence that S1 activity is gated based on the relevance of touch. However, our experiments do not rule out the possibility that the S1 activity resulting from our optogenetic stimulus differs between block types. A limitation of our tasks is that the tactile stimulus is unilateral whereas the visual stimulus is bilateral. In future work, our results should be compared with those using a version of our task with a unilateral visual stimulus. Our method of cortical inhibition relied on optogenetic excitation of parvalbumin-expressing cortical neurons, most of which are

GABAergic. However, a small fraction of glutamatergic pyramidal neurons also express parvalbumin[47,48] and may have been excited.

STAR★METHODS

RESOURCE AVAILABILITY

Lead contact—Further information and requests for resources and reagents should be directed to and will be fulfilled by the lead contact, Daniel H. O'Connor (dan.oconnor@jhmi.edu).

Materials availability—This study did not generate new unique reagents.

Data and code availability

- Data in MATLAB (.mat) and HDF5 (.h5) formats have been deposited at Zenodo and are publicly available as of the date of publication. DOIs are listed in the key resources table.
- All original code has been deposited at GitHub and is publicly available as of the date of publication. DOIs are listed in the key resources table.
- Any additional information required to reanalyze the data reported in this paper is available from the lead contact upon request.

EXPERIMENTAL MODEL AND STUDY PARTICIPANT DETAILS

Mice—All procedures were performed in accordance with protocols approved by the Johns Hopkins University Animal Care and Use Committee. Sixteen male and two female mice included in behavioral and optogenetic inhibition experiments were obtained by crossing PV-IRES-Cre (Jackson Labs: 008069; B6; 129P2-Pvalb$^{tm1(cre)Arbr}$/J)[49] with Ai32 (Jackson Labs: 012569; B6; 129S-Gt(ROSA) 26Sor$^{tm32(CAG—COP4*H134R/EYFP)Hze}$/J)[50] lines. Eleven male mice included in behavioral experiments were obtained by crossing SOM-IRES-Cre (Jackson Labs: 013044; Sst$^{tm2.1(cre)Zjh}$/J)[51] with Ai32 lines. Four male Emx1-Cre (Jackson Labs: 005628; B6.129S2-Emx1$^{tm1(cre)Krj}$/J)[52] mice included in optogenetic activation experiments were crossed with Ai32 mice. Three female C57BL/6 mice were included in high-speed video experiments. Mice ranged in age from 8 to 32 weeks and were housed in groups of up to five in a vivarium with reverse light-dark cycle (12 h each phase). Mice were singly housed after surgery and during behavioral experiments. Details of assignment to different experimental conditions are detailed in Table S1.

METHOD DETAILS

Behavioral task—All behavioral experiments were conducted with head-fixed mice. Behavioral apparatus was controlled by BControl software (C. Brody, Princeton University). Seven to 10 days after surgery and 7–14 days before behavioral training, mice were allowed ~1 mL of water daily until reaching ~70% of their starting body weight. On training days, mice were allowed to perform until sated and were weighed before and after each session to determine the amount of water consumed. Additional water was given if mice consumed <0.3 mL of water.

Stimulus-detection training—On the first day of training mice were acclimated to head fixation in the behavioral apparatus while being given free access to water via two reward ports located 6–10 mm and ~35° to the left and right of the mouse midline. On all subsequent training days, a single whisker (always on the right whisker pad) was threaded into a glass pipette attached to a piezo actuator (D220-A4-203YB, Piezo Systems), which was driven by a piezo controller (MDTC93B, Thorlabs). Approximately 1.5 mm of whisker remained exposed at the base. For ~1–3 days, mice were given a drop of water (~6 μL) for licking the right reward port after the onset of a tactile stimulus (sinusoidal deflections at 40 Hz, 1 s, ~1400 deg/s). Licks that occurred within a 0.1 s ‘‘grace period’’ immediately following stimulus onset were not rewarded. Licks that occurred in an ‘‘answer period’’ spanning 0.1 s–1.5 s after stimulus onset were rewarded. Licks occurring in a 0.2 s ‘‘censor period’’ ending at stimulus onset resulted in the withholding of the stimulus presentation for that trial and no reward or punishment. The length of the trial and the subsequent inter-trial interval remained the same despite the withholding of the stimulus. Trials with withheld stimuli were omitted from analysis. For the next ~1–3 days mice were presented with visual stimuli and given a drop of water for licking the left reward port until they began to reliably detect the stimuli. Each visual stimulus comprised 470 nm light (~5 mW, 1 s) generated by an LED (M470F1 LED driven by LEDD1B, Thorlabs) and emitted from the tip of an optic fiber (105 μm diameter, 0.22 NA; M43L01, Thorlabs) positioned 5.5 cm away from the tip of the mouse’s nose along its midline. Following this initial stimulus-detection training, training in the cross-modal selection task began.

Cross-modal selection task—In an initial stage of task training, mice were exposed to randomly interleaved trials (subject to a limit of 4 consecutive trials of the same type) in which each trial contained either one of two possible tactile stimuli (0.05 s or 0.15 s sinusoidal deflections at 20 Hz, ~800 deg/s) or one of two possible visual stimuli (0.05 s or 0.15 s flash, ~3 mW at tip of optic fiber). Stimulus onsets were separated by a random interval (3.5 s fixed interval + random interval drawn from an exponential distribution with 4 s mean). Within a session, trials were grouped into either respond-to-touch or respond-to-light blocks (~80 trials per block, 3–5 blocks per session). The grace, answer and censor periods were as described above for the stimulus-detection training. In respond-to-touch blocks, mice were rewarded with a drop of water for licking the reward port located to the right of the mouse following tactile but not visual stimuli. Mice were not rewarded if they licked the reward port located to the left of the mouse at any point within respond-to-touch blocks. In respond-to-light blocks, mice were rewarded if they licked the reward port located to the left of the mouse following visual but not tactile stimuli. They were not rewarded for licking the reward port located to the right of the mouse at any point during respond-to-light blocks. Blocks were not overtly signaled to the mouse (e.g., with a sensory cue) following a block switch. Instead, mice were allowed ~10 trials to begin responding to the correct stimulus modality through trial and error. If mice failed to switch after ~10 trials they were assisted via manual release of water at the correct reward port following a stimulus of the appropriate type.

After ~10–20 days of training, stimulus difficulty was increased (tactile: 0.05 s or 0.15 s sinusoidal deflections at 20 Hz, ~600 deg/s; visual: 0.05 s or 0.15 s flash attenuated to ~3

μW from the tip of the optic fiber using a neutral density filter; optical density = 3, NE530B, Thorlabs). Trials in which mice licked to the correct reward port following tactile stimuli in respond-to-touch blocks or visual stimuli in respond-to-light blocks were scored as ‘‘hit’’ trials. Failures to lick to the correct port after tactile stimuli in respond-to-touch blocks or visual stimuli in respond-to-light blocks were scored as ‘‘miss’’ trials. Licks to either reward port after tactile stimuli in respond-to-light blocks, visual stimuli in respond-to-touch blocks, or to the incorrect reward port after either stimulus type, resulted in ‘‘false alarm’’ trials. Trials in which mice correctly withheld licks after tactile stimuli in respond-to-light blocks, or after visual stimuli in respond-to-touch blocks, were scored as ‘‘correct rejection’’ trials. Performance was quantified as percent correct: 100*(# hits + # correct rejections)/(# of trials total). Training continued until mice achieved performance of >70% correct for at least two days. After reaching this performance criterion mice were given an additional ~17 test sessions for S1 recordings. Sessions in which overall performance was <65% correct, or <60% correct in either respond-to-touch blocks or respond-to-light blocks, were omitted from further analysis.

Cross-modal selection task with blocks to switch lick direction—In 4 mice previously trained on the standard cross-modal selection task, we introduced two additional block types during test sessions in order to switch the lick direction associated with tactile and visual stimuli (‘‘lick-direction-switch-task’’; Figure 4A). In respond-left-to-touch blocks, mice were rewarded for licking to the left reward port after tactile stimuli. No visual stimuli were presented, and no reward was given for licks to the right reward port. In respond-right-to-light blocks, mice were rewarded for licks to the right reward port after visual stimuli. No tactile stimuli were presented, and no reward was given for licks to the left reward port. Mice either began a test session with respond-left-to-touch and respond-right-to-light blocks that were followed by normal respond-right-to-touch/ignore-light and respond-left-to-light/ignore-touch blocks, or began a test session with normal respond-left-to-light/ignore-touch and respond-right-to-touch/ignore-light blocks followed by respond-left-to-touch and respond-right-to-light blocks.

Cross-modal selection task with more frequent block transitions—For the results shown in Figure S3, we modified the standard cross-modal selection task such that (1) the block length was approximately 60 trials and there were 4–7 blocks per session; and (2) a drop of water from the rewarded port was automatically released on the 9th trial following a block switch.

Tracking and analysis of whisker motion—One day prior to recording, most whiskers and non-whisker hairs on the right whisker pad were trimmed using fine forceps and scissors, under isoflurane (1.5%) anesthesia. The stimulated C2 whisker and a C3 or C4 ‘‘surrogate’’ whisker were retained but trimmed short. High-speed videos (500 Hz, 27 μm/pixel, 544 × 366 pixels) providing a bottom view of the right whisker pad, were acquired through a telecentric lens (0.25X, Edmund Optics), using a PhotonFocus DR1-D1312-200-G2-8 camera and Streampix 8 software (Norpix). Multiple parts of both whiskers in each video frame were annotated by a deep convolutional neural network, based on a pre-trained ResNet-50 using DeepLabCut[53,54]. After training the network using ~1000 manually labeled

frames sampled from all sessions, it was able to label whisker parts on test frames with an accuracy of 2.19 pixels. Whisker angles relative to the midline were calculated based on tracked points corresponding to the base and tip of the whisker. Whisker angle time series were median filtered (MATLAB ‘‘medfilt1’’, span of 10 frames). The amplitude of the whisker stimulus was determined as follows: first, the mean of the 100 ms period immediately preceding stimulus onset was subtracted from the stimulated whisker angle time series for each trial. The stimulus amplitude was then calculated for each trial as the mean of the 14–34 ms post-stimulus period. This time-period was chosen to isolate the peak of the first stimulus deflection. For whisker angle based ideal-observer analysis, we used MATLAB’s ‘‘perfcurve’’ function with baseline-subtracted (100 ms pre-stimulus baseline) data. A resulting AUC value was considered significant if its Bonferroni-corrected confidence interval did not include 0.5, with confidence level of each interval set for a family-wise false positive rate of 5% across 14 sessions. Pearson correlation coefficients were calculated using MATLAB ‘‘corrcoef’’.

Surgery

Microdrive implantation: Mice were implanted with titanium headposts.[40] Briefly, mice were anesthetized (1%–2% isoflurane in O_2; Surgivet) and mounted in a stereotaxic apparatus (David Kopf Instruments). Body temperature was maintained with a thermal blanket (Harvard Apparatus). The scalp and periosteum over the dorsal surface of the skull were removed. The skull surface over the posterior half of the left hemisphere which covers S1 was left untouched. The remaining exposed area of the skull was scored with a dental drill and the headpost affixed using cyanoacrylate adhesive (Krazy Glue) followed by dental acrylic (Jet Repair Acrylic). Mice were then implanted with a tetrode microdrive[55] coupled to an optic fiber (200 μm diameter, 0.39 NA) after we made a ~0.5 mm craniotomy. For S1 recordings, electrodes were targeted to −1.4 mm posterior and 3.8 mm lateral to bregma. Microdrives were fixed in place using dental acrylic.

Clear skull preparation: We adapted a clear skull preparation[27] for use in S1 optogenetic excitation and V1 inhibition experiments (described below). Modified headposts that exposed most of the dorsal surface of the skull were fixed to the skull using clear adhesive luting cement (C&B Metabond Quick Adhesive Cement System; Parkell). An additional layer of clear cement and in some cases a thin layer of cyanoacrylate glue (Krazy Glue) was applied to the entire surface of the exposed skull, leaving it largely transparent.

Electrophysiology

Tetrode recordings: For barrel cortex recordings in the cross-modal selection task, we recorded extracellularly from multiple neurons simultaneously using custom built 8-tetrode microdrives.[55] The tetrodes were fixed with cyanoacrylate adhesive to the side of an optic fiber (200 μm diameter, 0.39 NA) such that 900 μm extended past the fiber tip. The optic fiber was then itself fixed to the base of the microdrive using epoxy (5 min epoxy; Devcon). Microdrives were implanted into S1 at ~35° from vertical and as superficially as possible. After tetrode implantation, whiskers on the right whisker pad (contralateral to the left-hemisphere recording site) were manually stimulated while we monitored spiking activity. Whiskers that elicited the largest responses from the most neurons were used for

subsequent experiments while all other whiskers were trimmed to near their bases. After each day of recording in the cross-modal selection task we advanced the tetrodes ~75 μm to sample from a new set of neurons on the subsequent day of recording.

Silicon probe recordings: Linear 64-channel probes (ASSY-77 H3, Cambridge NeuroTech) were coated with DiI to histologically verify the site of recording post hoc. On the day of recording (>3 h before the start of recording), a craniotomy was made over left S1 (−1.4 mm posterior and 3.8 mm lateral to bregma) and subsequently covered with silicone elastomer (Kwik-Cast, WPI). The probe was inserted into the cortex at ~40° from vertical and left for 10 min before recording to allow for tissue relaxation. After silicon probe insertion, whiskers on the right whisker pad were manually stimulated while we monitored spiking activity. Whiskers that elicited the largest responses from the most neurons were used for subsequent experiments while all other whiskers were trimmed to near their bases. Neural signals and behavioral timestamps were recorded using an Intan system (RHD2000 series multi-channel amplifier chip; Intan Technologies).

S1 excitation—An optic fiber (200 μm diameter, 0.39 NA) coupled to a 473 nm wavelength laser (DHOM-L-473-200mW, UltraLasers) with intensity controlled by an acousto-optic modulator (MTS110-A3-VIS, QuantaTech) was used to deliver light for optogenetic stimulation to left S1 of Emx1-Cre; Ai32 mice with clear skull preparations. Mice were first trained on the cross-modal selection task. Two to three additional days of training were given in which 20% of tactile stimulus trials were replaced with trials where the laser stimulus was given alone but directed away from the skull of the mouse (‘‘sham’’ sessions; light was directed to the lower neck of the mouse instead). Blackout cloth and tape were used to shield the mouse’s eyes from scattered light resulting from the laser stimulus. Licking either reward port during these laser stimulus trials was not rewarded. Once it was confirmed that mice were not visually detecting the laser stimulus, ~3 optogenetic excitation sessions and ~3 sham sessions were given in an interleaved manner. During these sessions, the optic fiber was positioned such that its tip was ~2 mm above S1. Optogenetic excitation sessions followed the same procedure as the cross-modal selection task except that 20% of tactile stimulus trials were replaced with trials in which we instead delivered direct optogenetic stimulation of S1 (20 Hz sinusoidal wave, 0.15 s, ~3 mW peak power at the tip). Optogenetic stimulation trials were not rewarded. The interleaved sham sessions were nearly identical to optogenetic excitation sessions except that the fiber tip was retracted slightly (<1 mm) to fit blackout tape between it and the skull in order to block the laser light from reaching S1.

S1 or V1 inhibition

S1 inhibition.: PV-IRES-Cre; Ai32 mice implanted with optic-fiber-coupled microdrives in S1 were trained on the cross-modal task. An additional 2–3 training days were given in which laser stimuli (2–10 mW ramped down to 0 mW over 1.5 s) were delivered coincident with either the tactile or the visual stimulus (30% of trials), but with the laser decoupled from the implanted optic fiber. Decoupled fibers were left inside a protective cone that was used to protect the tetrode microdrives, and aimed at the dental acrylic on the mouse head. Blackout cloth and tape were used to shield the mouse’s eyes from scattered light due to the

laser. Once it was determined that mice did not reliably respond based on visual detection of the laser stimulus, 3–4 optogenetic inhibition sessions and 3–4 sham sessions were given in an interleaved manner. During optogenetic inhibition sessions, the laser was coupled to the implanted optic fiber. The trial structure of the sessions was identical to those in the cross-modal task except that laser stimuli (2–10 mW ramped down to 0 mW over 1.5 s) were delivered to left S1 in ~30% of tactile and visual stimulus trials. Onset of the laser stimulus was either simultaneous with the onset of tactile/visual stimuli or delayed by 50 ms. Additionally, in a subset of trials (~20%; ‘‘catch trials’’), laser stimuli were delivered alone, starting at the time that the onset of the tactile/visual stimuli would normally occur. Sham sessions were identical to optogenetic inhibition sessions except that the laser was decoupled from the implanted optic fiber in order to not inhibit S1.

V1 inhibition.: PV-IRES-Cre; Ai32 mice with clear skull preparations were first trained in the cross-modal task. Subsequent inhibition sessions were performed as described above for S1 inhibition, except that laser light was directed to visual cortex via optic fibers (200 μm diameter, 0.22 NA; TM200FL1B, Thorlabs) positioned over (~2 mm above) V1 bilaterally (3.5 mm posterior, ±2.5 mm lateral to the bregma; 8–10 mW each side). During sham-inhibition sessions, clear skull caps were covered by blackout cloth to not inhibit V1.

QUANTIFICATION AND STATISTICAL ANALYSIS

Electrophysiology—Broadband signals from all electrodes or probe contacts were filtered between 0.09 Hz and 7.6 kHz and sampled continuously at 30 kHz. Neural signals were bandpass filtered between either 300 Hz or 500 Hz and 6,000 Hz. Spikes from tetrode recordings were sorted using MClust software (A. David Redish). Spikes from silicon probe recordings were sorted using Kilosort.[56] Neurons were excluded from further analysis if the rate of ISI violations within a 2 ms window was >1%, L-ratios were >0.07. Neurons were also excluded if spike rates across a session showed a qualitatively obvious drift or if spike waveforms showed unstable shapes upon visual inspection.

Ideal-observer analysis

Detect probability (DP): A receiver operating characteristic (ROC) analysis was used to calculate DP for each neuron. DP was calculated by first binning (25 ms bins unless stated otherwise) the spiking activity for each neuron within tactile/visual stimulus trials (spikes aligned to stimulus onset). Next, trials were grouped by whether the mice licked a reward port (positive-label trials) or did not lick a reward port (negative-label trials) following a tactile/visual stimulus. Within each time bin a criterion spike rate was systematically varied (using ‘‘roc_auc_score’’ function from scikit-learn version 0.19.1 in Python 3) such that spike rates falling below the criterion were classified as negative trials while those falling above the criterion were classified as positive trials. At each criterion value, the classification of trials was compared to the true labels to calculate the false positive rate (FPR) and true positive rate (TPR). A ROC curve could then be constructed based on the FPR and TPR values. The area under the resulting ROC curve (AUC) corresponded to the DP for that time bin and neuron. To calculate 95% confidence intervals on the AUC for each neuron, we used a bootstrap procedure in which we resampled trials with replacement for each time bin.

Stimulus probability (SP): SP was calculated using a similar procedure as DP except that: (1) positive-label trials were those in which a tactile/visual stimulus was given and the mice did not make a lick response, and (2) we constructed negative-label trials by using a period during the intertrial interval in which there was no stimulus.

Detect probability onset: DP onset was considered to occur at the first of at least two consecutive time bins following a tactile/visual stimulus where the 95% confidence interval for DP did not include 0.5.

Modality preference index: A modality preference index was defined as:

$$\frac{\left|mean\ tactile\ DP\ -\ 0.5\right|\ -\ \left|mean\ visual\ DP\ -\ 0.5\right|}{\left|mean\ tactile\ DP\ -\ 0.5\right|+\left|mean\ visual\ DP\ -\ 0.5\right|}$$

where the tactile and visual DP means were taken over the first 500 ms after DP onset.

Statistics—Unless otherwise noted: we report data as mean ± SEM; statistical tests were two-tailed; statistical hypothesis testing used a = 0.05. Prior to using t-tests, we assessed normality using quantile-quantile plots. We chose statistical tests in the following order of decreasing preference: (1) parametric tests when appropriate (paired and unpaired t-tests); (2) non-parametric tests (sign-test); (3) randomization tests (permutation and bootstrap). If the tested sample was not symmetrical about its median, we used a sign test.

Unless otherwise noted, confidence intervals were calculated using a nonparametric multistage bootstrap method[57] that simulated the data generation process and incorporated variability both among behavioral sessions for a given mouse as well as across mice. The confidence interval for statistic Y (for example, mean difference between p(lick) for tactile trials with no manipulation and tactile optogenetic manipulation trials) was calculated by first separately pooling all trials of a given type (no-manipulation or manipulation) for each of N mice. This resulted in $N_{\mathrm{no-manip},k}$ no-manipulation trials and $N_{\mathrm{manip},k}$ manipulation trials for the $k-th$ mouse. Next, a set of N primary sampling units (PSU) was obtained by randomly sampling mice with replacement. $N_{\mathrm{no-manip},k}$ and $N_{\mathrm{manip},k}$ trials were then each randomly sampled with replacement for each PSU. Next, a bootstrap replicate Y^* was calculated from these resampled trials. This process was repeated 10,000 times to obtain a set of Y^* bootstrapped replicates. The 95% confidence interval was calculated using the 2.5th and 97.5th percentile values of Y^*.

We assigned mice of appropriate genotypes to experimental groups arbitrarily, without randomization or blinding. We did not use statistical methods to predetermine sample sizes. Sample sizes are similar to those reported in the field.

Supplementary Material

Refer to Web version on PubMed Central for supplementary material.

ACKNOWLEDGMENTS

We thank Solange Brown, Maxime Cheveé, Shreesh Mysore, and Veit Stuphorn for comments. Supported by the Whitehall Foundation (D.H.O.), Klingenstein Fund (D.H.O.), Johns Hopkins Science of Learning Institute (D.H.O.), and NIH grants R01NS089652 (D.H.O.), 1R01NS104834-01 (D.H.O., J.Y.C.), and P30NS050274.

REFERENCES

1. Norman DA, and Shallice T (1986). Attention to Action: Willed and Automatic Control of Behavior. In Consciousness and Self-Regulation: Advances in Research and Theory, Davidson RJ, Schwartz GE, and Shapiro D, eds. (Springer Science+Business Media), pp. 1–18.
2. Moore T, and Zirnsak M (2017). Neural Mechanisms of Selective Visual Attention. Annu. Rev. Psychol. 68, 47–72. 10.1146/annurev-psych-122414-033400. [PubMed: 28051934]
3. Rizzolatti G, Riggio L, Dascola I, and Umiltá C (1987). Reorienting attention across the horizontal and vertical meridians: evidence in favor of a premotor theory of attention. Neuropsychologia 25, 31–40. 10.1016/0028-3932(87)90041-8. [PubMed: 3574648]
4. Moore T, and Armstrong KM (2003). Selective gating of visual signals by microstimulation of frontal cortex. Nature 421, 370–373. 10.1038/nature01341. [PubMed: 12540901]
5. Moore T, and Fallah M (2001). Control of eye movements and spatial attention. Proc. Natl. Acad. Sci. USA 98, 1273–1276. 10.1073/pnas.021549498. [PubMed: 11158629]
6. Moore T, Armstrong KM, and Fallah M (2003). Visuomotor origins of covert spatial attention. Neuron 40, 671–683. 10.1016/s0896-6273(03)00716-5. [PubMed: 14622573]
7. Winkowski DE, and Knudsen EI (2007). Top-down control of multimodal sensitivity in the barn owl optic tectum. J. Neurosci. 27, 13279–13291. 10.1523/JNEUROSCI.3937-07.2007. [PubMed: 18045922]
8. Winkowski DE, and Knudsen EI (2008). Distinct mechanisms for top-down control of neural gain and sensitivity in the owl optic tectum. Neuron 60, 698–708. 10.1016/j.neuron.2008.09.013. [PubMed: 19038225]
9. Cheveé M, Finkel EA, Kim S-J, O'Connor DH, and Brown SP (2022). Neural activity in the mouse claustrum in a cross-modal sensory selection task. Neuron 110, 486–501.e7. 10.1016/j.neuron.2021.11.013. [PubMed: 34863367]
10. Kwon SE, Yang H, Minamisawa G, and O'Connor DH (2016). Sensory and decision-related activity propagate in a cortical feedback loop during touch perception. Nat. Neurosci. 19, 1243–1249. 10.1038/nn.4356. [PubMed: 27437910]
11. Le Merre P, Esmaeili V, Charrière E, Galan K, Salin P-A, Petersen CCH, and Crochet S (2018). Reward-Based Learning Drives Rapid Sensory Signals in Medial Prefrontal Cortex and Dorsal Hippocampus Necessary for Goal-Directed Behavior. Neuron 97, 83–91.e5. 10.1016/j.neuron.2017.11.031. [PubMed: 29249287]
12. Sachidhanandam S, Sreenivasan V, Kyriakatos A, Kremer Y, and Petersen CCH (2013). Membrane potential correlates of sensory perception in mouse barrel cortex. Nat. Neurosci. 16, 1671–1677. 10.1038/nn.3532. [PubMed: 24097038]
13. Takahashi N, Oertner TG, Hegemann P, and Larkum ME (2016). Active cortical dendrites modulate perception. Science 354, 1587–1590. 10.1126/science.aah6066. [PubMed: 28008068]
14. Yamashita T, and Petersen CC (2016). Target-specific membrane potential dynamics of neocortical projection neurons during goal-directed behavior. Elife 5, e15798. 10.7554/eLife.15798. [PubMed: 27328320]
15. Yang H, Kwon SE, Severson KS, and O'Connor DH (2016). Origins of choice-related activity in mouse somatosensory cortex. Nat. Neurosci. 19, 127–134. 10.1038/nn.4183. [PubMed: 26642088]
16. Foffani G, and Moxon KA (2004). PSTH-based classification of sensory stimuli using ensembles of single neurons. J. Neurosci. Methods 135, 107–120. 10.1016/j.jneumeth.2003.12.011. [PubMed: 15020095]
17. O'Connor DH, Peron SP, Huber D, and Svoboda K (2010). Neural activity in barrel cortex underlying vibrissa-based object localization in mice. Neuron 67, 1048–1061. 10.1016/j.neuron.2010.08.026. [PubMed: 20869600]

18. Sandler AJ (2008). Chronic Recording During Learning. In Methods for Neural Ensemble Recordings Frontiers in Neuroscience, Nicolelis MA, ed. (CRC Press/Taylor & Francis), pp. 125–143.
19. Britten KH, Newsome WT, Shadlen MN, Celebrini S, and Movshon JA (1996). A relationship between behavioral choice and the visual responses of neurons in macaque MT. Vis. Neurosci. 13, 87–100. 10.1017/s095252380000715x. [PubMed: 8730992]
20. Nienborg H, Cohen MR, and Cumming BG (2012). Decision-related activity in sensory neurons: correlations among neurons and with behavior. Annu. Rev. Neurosci. 35, 463–483. 10.1146/annurev-neuro-062111-150403. [PubMed: 22483043]
21. Drew PJ, Winder AT, and Zhang Q (2019). Twitches, Blinks, and Fidgets: Important Generators of Ongoing Neural Activity. Neuroscientist 25, 298–313. 10.1177/1073858418805427. [PubMed: 30311838]
22. Musall S, Kaufman MT, Juavinett AL, Gluf S, and Churchland AK (2019). Single-trial neural dynamics are dominated by richly varied movements. Nat. Neurosci. 22, 1677–1686. 10.1038/s41593-019-0502-4. [PubMed: 31551604]
23. Parker PRL, Brown MA, Smear MC, and Niell CM (2020). Movement-Related Signals in Sensory Areas: Roles in Natural Behavior. Trends Neurosci. 43, 581–595. 10.1016/j.tins.2020.05.005. [PubMed: 32580899]
24. Steinmetz NA, Zatka-Haas P, Carandini M, and Harris KD (2019). Distributed coding of choice, action and engagement across the mouse brain. Nature 576, 266–273. 10.1038/s41586-019-1787-x. [PubMed: 31776518]
25. Stringer C, Pachitariu M, Steinmetz N, Reddy CB, Carandini M, and Harris KD (2019). Spontaneous behaviors drive multidimensional, brainwide activity. Science 364, 255. 10.1126/science.aav7893. [PubMed: 31000656]
26. Zagha E, Erlich JC, Lee S, Lur G, O'Connor DH, Steinmetz NA, Stringer C, and Yang H (2022). The importance of accounting for movement when relating neuronal activity to sensory and cognitive processes. JN-TS-1919-21 (J Neurosci). 10.1523/JNEUROSCI.1919-21.2021.
27. Guo ZV, Li N, Huber D, Ophir E, Gutnisky D, Ting JT, Feng G, and Svoboda K (2014). Flow of cortical activity underlying a tactile decision in mice. Neuron 81, 179–194. 10.1016/j.neuron.2013.10.020. [PubMed: 24361077]
28. Resulaj A, Ruediger S, Olsen SR, and Scanziani M (2018). First spikes in visual cortex enable perceptual discrimination. Elife 7, e34044. 10.7554/eLife.34044. [PubMed: 29659352]
29. Auffret M, Ravano VL, Rossi GMC, Hankov N, Petersen MFA, and Petersen CCH (2018). Optogenetic stimulation of cortex to map evoked whisker movements in awake head-restrained mice. Neuroscience 368, 199–213. 10.1016/j.neuroscience.2017.04.004. [PubMed: 28412497]
30. Matyas F, Sreenivasan V, Marbach F, Wacongne C, Barsy B, Mateo C, Aronoff R, and Petersen CCH (2010). Motor control by sensory cortex. Science 330, 1240–1243. 10.1126/science.1195797. [PubMed: 21109671]
31. Petersen CCH (2014). Cortical control of whisker movement. Annu. Rev. Neurosci. 37, 183–203. 10.1146/annurev-neuro-062012-170344. [PubMed: 24821429]
32. von Heimendahl M, Itskov PM, Arabzadeh E, and Diamond ME (2007). Neuronal activity in rat barrel cortex underlying texture discrimination. PLoS Biol. 5, e305. 10.1371/journal.pbio.0050305. [PubMed: 18001152]
33. Isett BR, Feasel SH, Lane MA, and Feldman DE (2018). Slip-Based Coding of Local Shape and Texture in Mouse S1. Neuron 97, 418–433.e5. 10.1016/j.neuron.2017.12.021. [PubMed: 29307709]
34. Knutsen PM, Pietr M, and Ahissar E (2006). Haptic object localization in the vibrissal system: behavior and performance. J. Neurosci. 26, 8451–8464. 10.1523/JNEUROSCI.1516-06.2006. [PubMed: 16914670]
35. Mehta SB, Whitmer D, Figueroa R, Williams BA, and Kleinfeld D (2007). Active spatial perception in the vibrissa scanning sensorimotor system. PLoS Biol. 5, e15. 10.1371/journal.pbio.0050015. [PubMed: 17227143]

36. O'Connor DH, Clack NG, Huber D, Komiyama T, Myers EW, and Svoboda K (2010). Vibrissa-based object localization in head-fixed mice. J. Neurosci. 30, 1947–1967. 10.1523/JNEUROSCI.3762-09.2010. [PubMed: 20130203]
37. Petreanu L, Gutnisky DA, Huber D, Xu N.l., O'Connor DH, Tian L, Looger L, and Svoboda K (2012). Activity in motor-sensory projections reveals distributed coding in somatosensation. Nature 489, 299–303. 10.1038/nature11321. [PubMed: 22922646]
38. Ranganathan GN, Apostolides PF, Harnett MT, Xu N-L, Druckmann S, and Magee JC (2018). Active dendritic integration and mixed neocortical network representations during an adaptive sensing behavior. Nat. Neurosci. 21, 1583–1590. 10.1038/s41593-018-0254-6. [PubMed: 30349100]
39. Xu N.l., Harnett MT, Williams SR, Huber D, O'Connor DH, Svoboda K, and Magee JC (2012). Nonlinear dendritic integration of sensory and motor input during an active sensing task. Nature 492, 247–251. 10.1038/nature11601. [PubMed: 23143335]
40. O'Connor DH, Hires SA, Guo ZV, Li N, Yu J, Sun Q-Q, Huber D, and Svoboda K (2013). Neural coding during active somatosensation revealed using illusory touch. Nat. Neurosci. 16, 958–965. 10.1038/nn.3419. [PubMed: 23727820]
41. Mayrhofer JM, El-Boustani S, Foustoukos G, Auffret M, Tamura K, and Petersen CCH (2019). Distinct Contributions of Whisker Sensory Cortex and Tongue-Jaw Motor Cortex in a Goal-Directed Sensorimotor Transformation. Neuron 103, 1034–1043.e5. 10.1016/j.neuron.2019.07.008. [PubMed: 31402199]
42. Oude Lohuis MN, Pie JL, Marchesi P, Montijn JS, de Kock CPJ, Pennartz CMA, and Olcese U (2022). Multisensory task demands temporally extend the causal requirement for visual cortex in perception. Nat. Commun. 13, 2864. 10.1038/s41467-022-30600-4. [PubMed: 35606448]
43. Hong YK, Lacefield CO, Rodgers CC, and Bruno RM (2018). Sensation, movement and learning in the absence of barrel cortex. Nature 561, 542–546. 10.1038/s41586-018-0527-y. [PubMed: 30224746]
44. Hutson KA, and Masterton RB (1986). The sensory contribution of a single vibrissa's cortical barrel. J. Neurophysiol. 56, 1196–1223. 10.1152/jn.1986.56.4.1196. [PubMed: 3783236]
45. Kurnikova A, Moore JD, Liao S-M, Deschênes M, and Kleinfeld D (2017). Coordination of Orofacial Motor Actions into Exploratory Behavior by Rat. Curr. Biol. 27, 688–696. 10.1016/j.cub.2017.01.013. [PubMed: 28216320]
46. Welker WI (1964). Analysis of Sniffing of the Albino Rat 1). Beyond Behav. 22, 223–244. 10.1163/156853964X00030.
47. Tanahira C, Higo S, Watanabe K, Tomioka R, Ebihara S, Kaneko T, and Tamamaki N (2009). Parvalbumin neurons in the forebrain as revealed by parvalbumin-Cre transgenic mice. Neurosci. Res. 63, 213–223. 10.1016/j.neures.2008.12.007. [PubMed: 19167436]
48. Jinno S, and Kosaka T (2004). Parvalbumin is expressed in glutamatergic and GABAergic corticostriatal pathway in mice. J. Comp. Neurol. 477, 188–201. 10.1002/cne.20246. [PubMed: 15300789]
49. Hippenmeyer S, Vrieseling E, Sigrist M, Portmann T, Laengle C, Ladle DR, and Arber S (2005). A developmental switch in the response of DRG neurons to ETS transcription factor signaling. PLoS Biol. 3, e159. 10.1371/journal.pbio.0030159. [PubMed: 15836427]
50. Madisen L, Mao T, Koch H, Zhuo J.m., Berenyi A, Fujisawa S, Hsu Y-WA, Garcia AJ, Gu X, Zanella S, et al. (2012). A toolbox of Cre-dependent optogenetic transgenic mice for light-induced activation and silencing. Nat. Neurosci. 15, 793–802. 10.1038/nn.3078. [PubMed: 22446880]
51. Taniguchi H, He M, Wu P, Kim S, Paik R, Sugino K, Kvitsiani D, Fu Y, Lu J, Lin Y, et al. (2011). A resource of Cre driver lines for genetic targeting of GABAergic neurons in cerebral cortex. Neuron 71, 995–1013. 10.1016/j.neuron.2011.07.026. [PubMed: 21943598]
52. Gorski JA, Talley T, Qiu M, Puelles L, Rubenstein JLR, and Jones KR (2002). Cortical excitatory neurons and glia, but not GABAergic neurons, are produced in the Emx1-expressing lineage. J. Neurosci. 22, 6309–6314. . [PubMed: 12151506]
53. Mathis A, Mamidanna P, Cury KM, Abe T, Murthy VN, Mathis MW, and Bethge M (2018). DeepLabCut: markerless pose estimation of user-defined body parts with deep learning. Nat. Neurosci. 21, 1281–1289. 10.1038/s41593-018-0209-y. [PubMed: 30127430]

54. Nath T, Mathis A, Chen AC, Patel A, Bethge M, and Mathis MW (2019). Using DeepLabCut for 3D markerless pose estimation across species and behaviors. Nat. Protoc. 14, 2152–2176. 10.1038/s41596-019-0176-0. [PubMed: 31227823]

55. Cohen JY, Haesler S, Vong L, Lowell BB, and Uchida N (2012). Neuron-type-specific signals for reward and punishment in the ventral tegmental area. Nature 482, 85–88. 10.1038/nature10754. [PubMed: 22258508]

56. Pachitariu M, Steinmetz N, Kadir S, Carandini M, and Kenneth D H (2016). Kilosort: realtime spike-sorting for extracellular electrophysiology with hundreds of channels. Preprint at bioRxiv, 061481. 10.1101/061481.

57. Davison AC, and Hinkley DV (1997). Bootstrap Methods and Their Application (Cambridge University Press).

Highlights

- A tactile-visual cross-modal selection task for head-fixed mice
- Sensory and motor activity interact in S1 to promote tactile detection
- S1 activity is gated based on the relevance of touch vs. vision

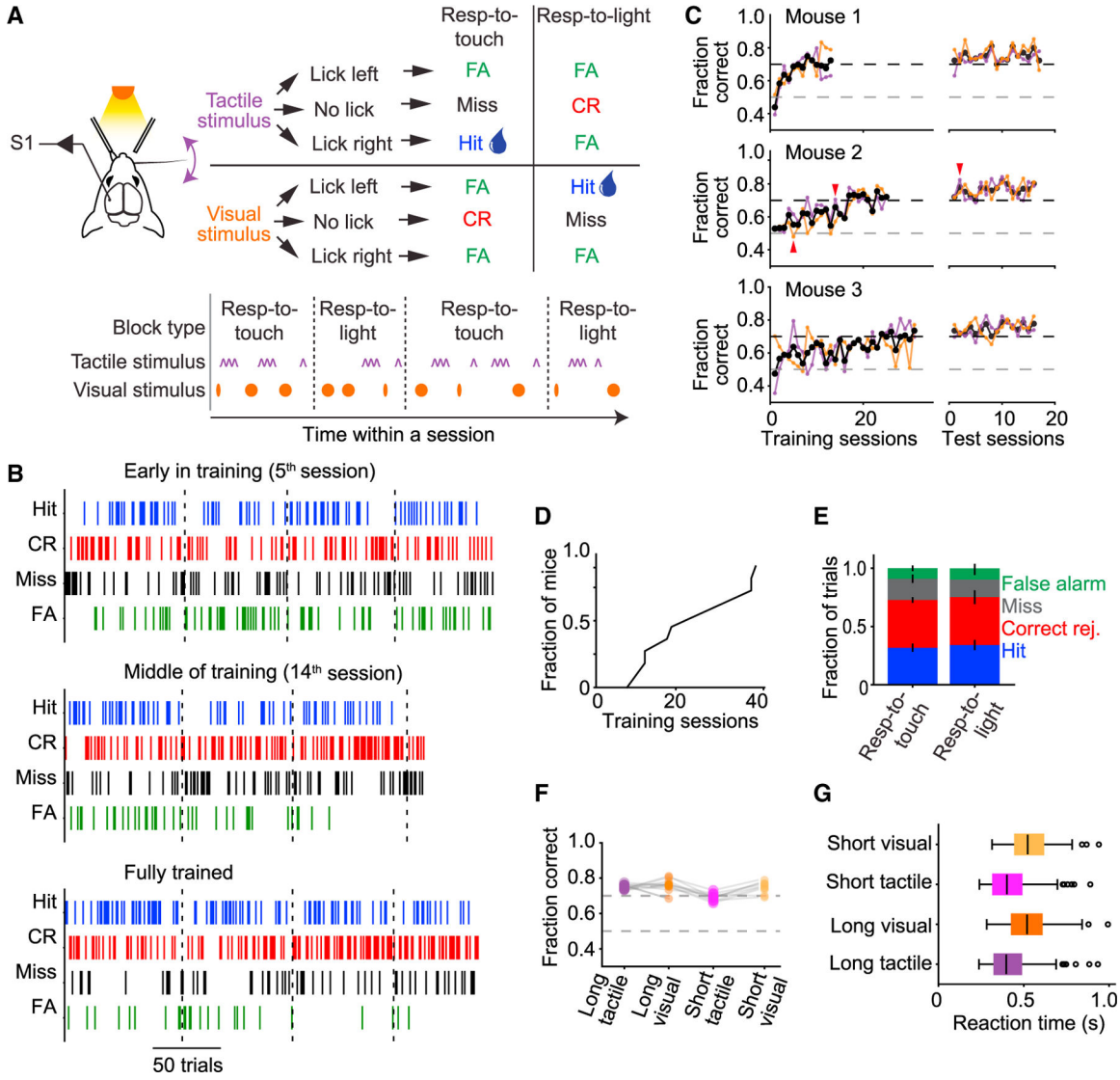

Figure 1. A cross-modal selection task for head-fixed mice

(A) Tactile and visual stimuli were randomly interleaved throughout a behavioral session, grouped into respond-to-touch and respond-to-light blocks of trials that alternated (3–5 per session, ~80 trials each). Mice were rewarded with a drop of water for licking a reward port located to the right of the mouse after a tactile stimulus in a respond-to-touch block, or for licking a reward port located to the left of the mouse after a visual stimulus in a respond-to-light block. No reward was given for licking either port after a tactile stimulus in a respond-to-light block or after a visual stimulus in a respond-to-touch block.

(B) Behavioral performance in an early training session (5th session; top), in a session in the middle of training (14th session; middle), and after training (2nd test session; bottom). Colored ticks represent the occurrence of the four types of trial outcome over the course of a session.

(C) Performance of three example mice during training and testing periods. Overall performance is indicated by black traces, performance in respond-to-touch blocks by purple traces, and performance in respond-to-light blocks by orange traces. After training, an

additional ~17 test sessions with the same task design were given; test sessions where performance fell below criterion were excluded and not used in later analyses (red arrows mark sessions in B).

(D) Time to criterion performance (70% correct for 2 days) across mice (median 19).

(E) Fractions of trial outcomes were similar across respond-to-touch and respond-to-light blocks (error bars denote ± SEM).

(F) Performance was similar across all stimulus types for all mice.

(G) Reaction-time distributions across the different stimulus types. Black vertical lines indicate medians, boxes indicate interquartile range (IQR), whiskers indicate 1.53 IQR, and circles indicate outliers.

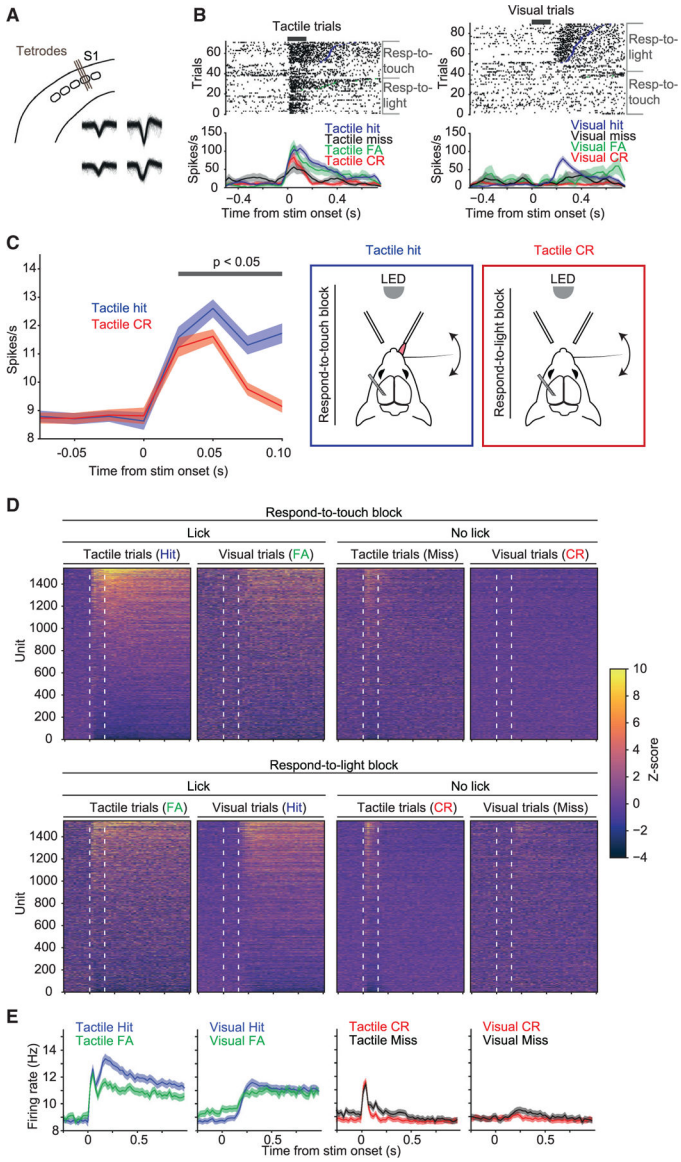

Figure 2. Relevance-dependent tactile and motor activity in S1

(A) Extracellular single-unit activity was recorded in whisker S1 (barrel) cortex using 32-channel tetrode microdrives.

(B) Raster plots (top) and peristimulus spike time histograms (PSTHs, bottom; 25-ms bins, mean ± SEM) for an example unit. Rasters and PSTHs are aligned to the onset of either the long tactile stimuli (left, ‘‘tactile trials’’) or the long visual stimuli (right, ‘‘visual trials’’) and sorted by block and trial outcome. Thick black bars indicate period of stimulus delivery.

(C) Mean population responses to the tactile stimulus were larger when the stimulus occurred in a respond-to-touch block and resulted in the mouse correctly making a lick response (tactile hits; blue curve) compared with when the stimulus occurred in a respond-to-light block and the mouse correctly withheld licking (tactile correct rejections; red curve). This difference in activity was evident as soon as 25 ms after stimulus onset. Error shading

denotes ±SEM. Gray bar indicates time bins where $p < 0.05$ from tests performed in Figure S1. Schematics of the two trial types are shown in panels on the right.

(D) Normalized activity across the population of recorded neurons (n = 1,539 units from 11 mice). Trials are grouped by block type, stimulus type, and trial outcome and sorted by mean activity during a 500-ms window after stimulus onset in tactile hits. White dashed lines indicate the onset and offset of the long tactile or visual stimuli.

(E) Mean PSTHs across all 1,539 neurons for each of the four types of trial outcome (Hit, FA, CR, Miss) for both stimulus types (tactile, visual). Error shading denotes ± SEM.

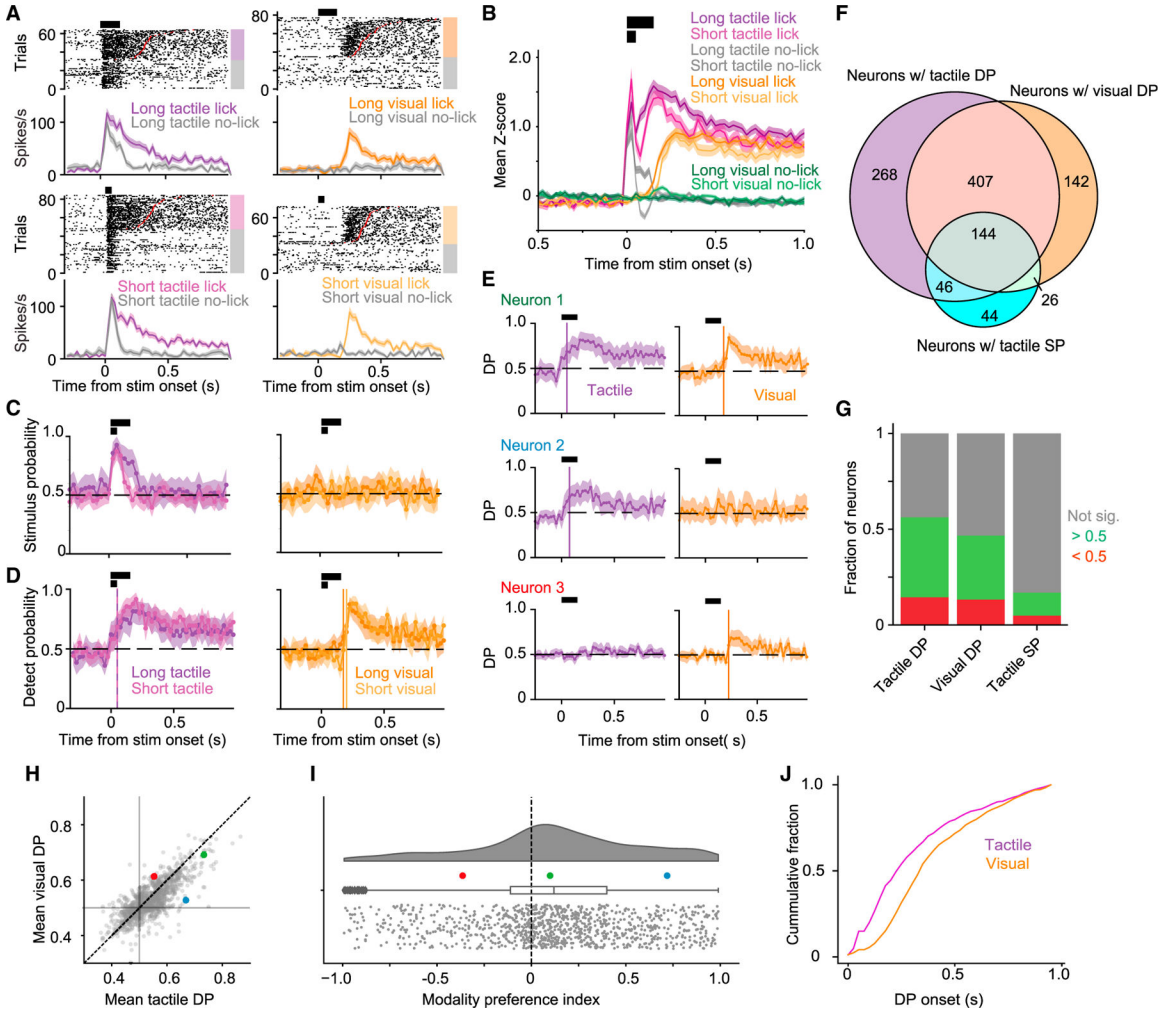

Figure 3. Trial-by-trial encoding of touch and lick actions

(A) Raster plots and PSTHs (mean ± SEM, 25-ms bins) for an example neuron separately for long (150 ms; top row) and short (50 ms; bottom row) tactile (left column) and visual (right column) stimuli. Trials are grouped by whether the mouse licked. Increased activity is evident in association with the tactile stimulus, licking after the tactile stimulus, and licking after the visual stimulus, but not with the visual stimulus.

(B) Mean normalized activity (±SEM, 25-ms bins) of all neurons recorded (n = 1,539 units from 11 mice) across stimulus trials with a lick response. Horizontal black bars indicate periods of short and long stimulus delivery.

(C) Stimulus probability (SP) for the example neuron in (A) (mean ± 95% confidence interval [CI], 25-ms bins). Significant (95% CI > 0.5) SP was prolonged for long (dark purple) relative to short (light purple) tactile stimulus trials, and not evident for either long (dark orange) or short (light orange) visual stimulus trials.

(D) Detect probability (DP) for the example neuron in (A) (mean ± 95% CI, 25-ms bins). Significant (95% CI > 0.5) DP was detected for long and short tactile and visual stimulus trials. Vertical colored lines indicate onset of significant DP for the different trial types.

(E) Three example neurons illustrating range of DP responses (mean ± 95% CI, 25-ms bins). Neurons could show significant DP for both tactile and visual trials (top), for only tactile lick trials (middle), or for only visual lick trials (bottom).

(F) Overlap of neurons with significant values (95% CI does not include 0.5 for two consecutive bins after stimulus onset) of DP in tactile trials, DP in visual trials, or SP in tactile trials.

(G) Fractions of neurons with significant positive-going (green), negative-going (red), or no (gray) significant DP and SP (n = 1,539 units from 11 mice).

(H) Mean tactile vs. visual DP values for each unit with significant values of both. Symbols show mean over the first 500 ms following onset of significant DP. Colored symbols indicate example neurons in (E).

(I) Distribution of modality preference index for units with significant values of both tactile and visual DP. Box plot indicates median, IQR, and 1.5× IQR (whiskers).

(J) Cumulative distributions of the time of DP onset with respect to stimulus onset for tactile (purple) and visual (orange) trials.

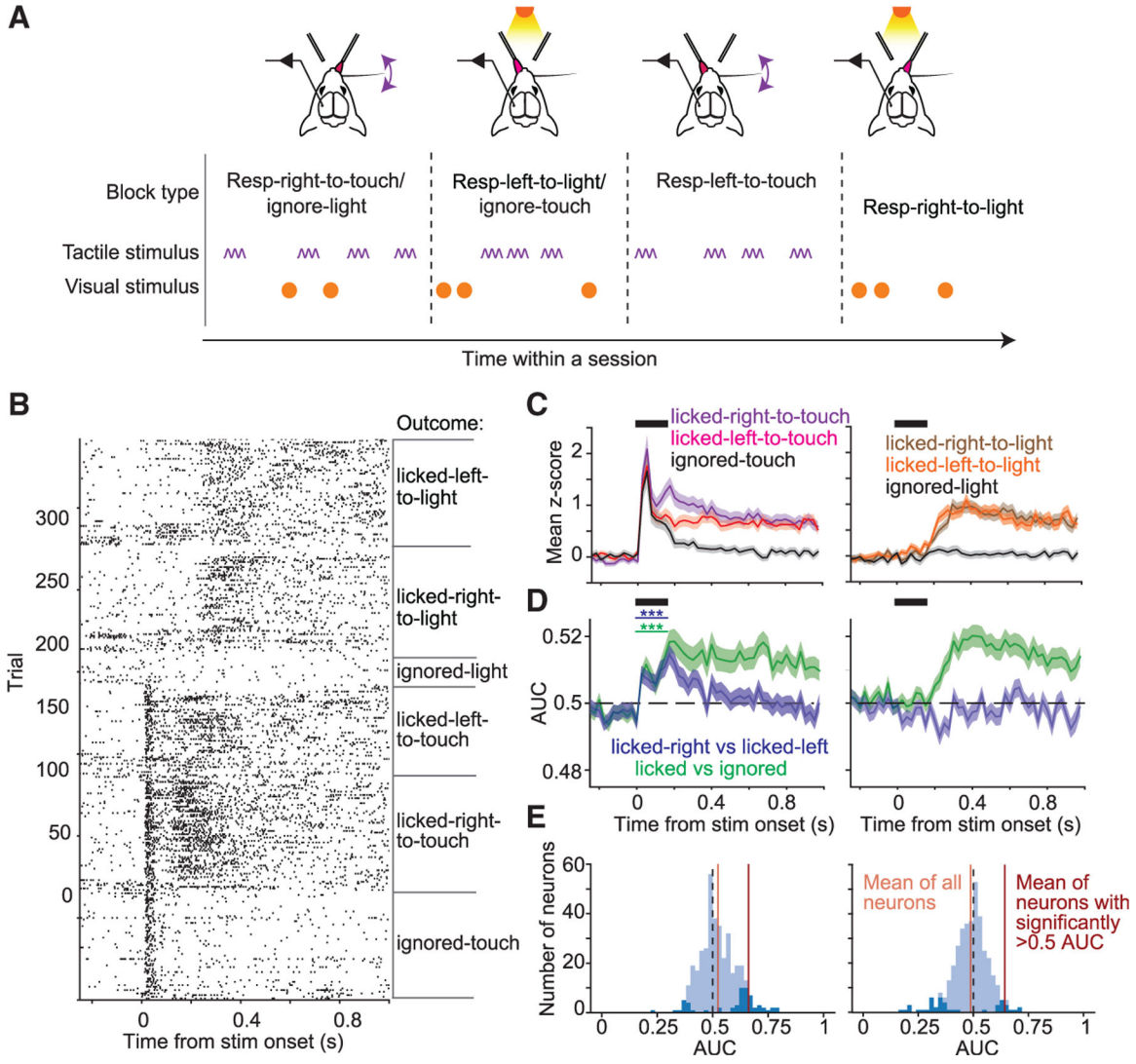

Figure 4. Sensory-motor integration in S1

(A) Cross-modal selection task with added blocks of trials to control for lick direction. Two additional block types were added to test sessions for mice trained on the cross-modal selection task, one in which mice were given only tactile stimuli and rewarded for licking left (‘‘respond-left-to-touch’’ trials) and one in which mice were given only visual stimuli and rewarded for licking right (‘‘respond-right-to-light’’ trials).

(B) Raster plot for an example neuron sorted by stimulus type and trial outcome.

(C) Mean normalized PSTHs (±SEM) for tactile (left) and visual (right) trials, grouped by lick outcome (ignore, lick-left, or lick-right).

(D) Left: mean area under the ROC curve (AUC) (±SEM) for discriminating respond-to-touch vs. ignore trials (green traces, $p < 1 \times 10^{-3}$, one-sided one-sample t test on first 150-ms bin, $n = 375$ neurons) or licked-right vs. licked-left trials (blue traces, $p < 1 \times 10^{-3}$). Right: same as left but for respond-to-light trials.

(E) Distributions of AUC for individual neurons. Dark-blue bars indicate neurons with significant AUC values. Left: mean AUC values (over first 150 ms after stimulus onset)

for licked-right-to-touch vs. licked-left-to-touch comparison. Right: similar to left but for licked-right-to-light vs. licked-left-to-light.

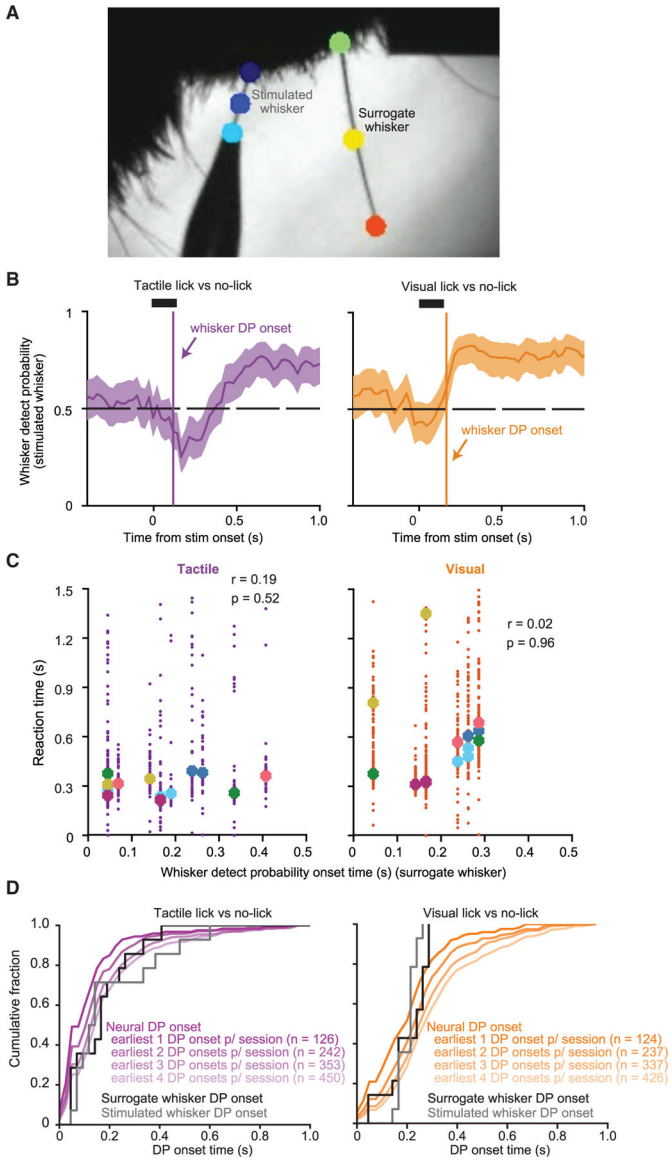

Figure 5. Motor activity in S1 cannot be explained by whisker motion

(A) Example high-speed video frame showing the stimulated whisker (threaded into the stimulator pipette) and a ‘‘surrogate’’ whisker used to monitor whisking. Other whiskers were trimmed. Points on the whiskers (colored circles) were tracked to quantify whisker position and motion.

(B) ‘‘Whisker detect probability’’ (mean ± 95% CI) for the stimulated whisker.

(C) Reaction time for each trial plotted against that session’s surrogate whisker DP onset time for tactile hit (left) and visual hit (right) trials. Median reaction time for each session is indicated, color coded by mouse. Pearson correlation coefficients and corresponding *p* values are indicated.

(D) Cumulative histograms of whisker DP onset times for each session (black and gray curves), plotted for comparison with cumulative histograms of the earliest neural DP onsets for each session, for tactile (left, purple curves) and visual (right, orange curves) stimuli. The

different neural DP curves (shades of purple and orange) show results based on defining the ‘‘earliest’’ DP onsets as including only that of the single earliest neuron, as including the two earliest neurons, three earliest, and so on. The total number of neurons included in each histogram is indicated in parentheses.

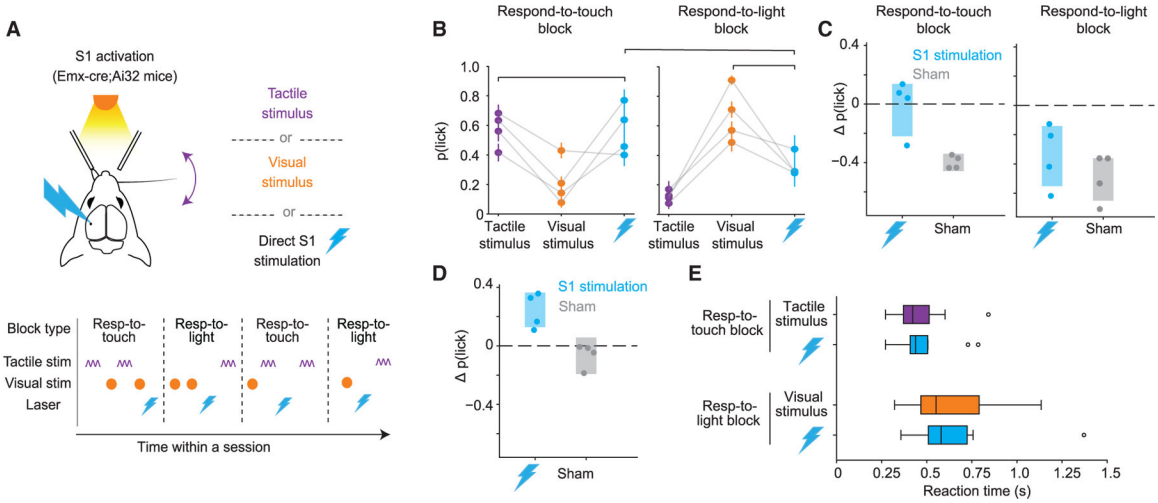

Figure 6. S1 excitation promotes lick responses during respond-to-touch but not respond-to-light blocks

(A) Direct optogenetic excitation of S1 replaced either tactile or visual stimuli in 20% of test-session trials in the cross-modal selection task.

(B) Probability that mice licked for each trial type during respond-to-touch (left) and respond-to-light (right) blocks. Brackets indicate comparisons shown in (C) and (D). Error bars denote ± SEM.

(C) Left: difference in p(lick) after direct excitation of S1 vs. after tactile stimuli in respond-to-touch blocks (groups indicated by leftmost bracket in B) for four mice. Sham trials are from days in which mice underwent the same experiment as in (A) but with laser illumination of S1 obstructed. Right: similar to left panel but comparing p(lick) after direct excitation of S1 vs. after visual stimuli in respond-to-light blocks. Shaded regions indicate 95% CI for the mean Δp(lick). Excitation of S1 elicited licking at comparable levels to tactile stimuli in respond-to-touch blocks but did not elicit licking at comparable levels to visual stimuli in respond-to-light blocks.

(D) Similar to (C) but comparing p(lick) after direct excitation of S1 in respond-to-touch blocks vs. respond-to-light blocks (groups indicated by topmost bracket in B). Excitation of S1 during respond-to-touch blocks elicited licking at a higher level than in respond-to-light blocks.

(E) Box plots depicting reaction times for correct lick responses to tactile or visual stimuli as well as for lick responses to direct optogenetic stimulation of S1 in respond-to-touch blocks or respond-to-light blocks. Vertical lines indicate medians, boxes indicate IQR, whiskers indicate 1.5× IQR, and circles indicate outliers. Reaction times to direct excitation of S1 are more similar to reaction times to tactile stimulation in respond-to-touch blocks than in respond-to-light blocks.

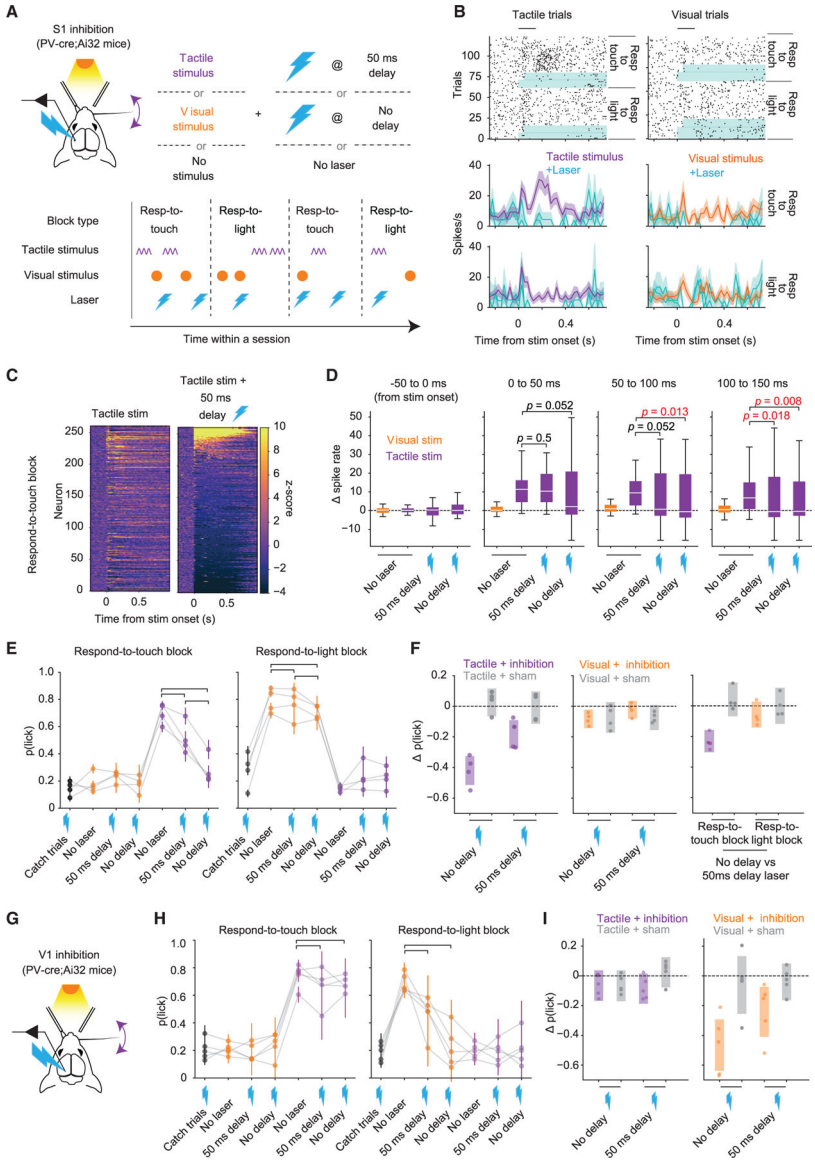

Figure 7. Inhibiting S1 activity selectively impairs tactile detection

(A) Optogenetic inhibition (lightning bolts) occurred in 30% of test-session trials, beginning simultaneously or with a 50-ms delay relative to the onset of the tactile or visual stimulus.

(B) Raster plots and PSTHs (mean ± SEM) for an example neuron during inhibition trials or normal tactile and visual trials (blue highlight indicates periods of inhibition).

(C) Heatmap of *Z*-scored activity across all neurons ($n = 261$ from four mice).

(D) Change in spike rate relative to baseline for neurons with a significant positive-going (>0.5) SP in respond-to-touch blocks. The effect of inhibition was delayed in the ‘‘50 ms delay’’ condition relative to the ‘‘no delay’’ condition (*p* values are from sign tests; horizontal lines, medians; boxes, IQR; whiskers, 1.5× IQR; outliers not depicted for clarity).

(E) Behavioral effects of S1 inhibition for different trial types in respond-to-touch (left) or respond-to-light (right) blocks. ‘‘Catch’’ trials are those with inhibition but no tactile or visual stimulus. Brackets indicate conditions compared in (F). Inhibition of S1 during tactile

stimuli in respond-to-touch blocks led to a decrease in the probability of licking. Inhibition of S1 during a visual stimulus in respond-to-light blocks did not lead to an obvious change in the probability of licking. Error bars denote ±SEM.

(F) Left: difference in p(lick) after tactile + inhibition trials vs. tactile (no laser) trials (data indicated by brackets from left panel in E). Sham trials are from days in which mice underwent the same experiment as in (A) but with laser illumination of S1 obstructed. Middle: similar to left panel but comparing p(lick) after visual + inhibition trials vs. visual (no laser) trials (data indicated by brackets from right panel in E). Right: similar to left panel but for tactile/visual + no delay inhibition vs. tactile/visual +50 ms delay inhibition. Shaded regions indicate 95% CI on Δp(lick).

(G) Schematic of V1 inhibition experiment.

(H) Similar to (E) but showing effects of inhibition of V1.

(I) Similar to left and middle panels of (F) but for V1 inhibition.

KEY RESOURCES TABLE

REAGENT or RESOURCE	SOURCE	IDENTIFIER
Chemicals, peptides, and recombinant proteins		
Isoflurane	Penn Veterinary	VED1360CS
Dental acrylic	Jet Repair Acrylic	L25-0335
Clear adhesive luting cement	Parkell	S399
Dil Stain	Thermo Fisher Scientific	D282
Silicone elastomer	World Precision Instruments	KWIK-CAST
Deposited data		
Data in MATLAB (.mat) and HDF5 (.h5) format for this paper	Zenodo	Zenodo: https://doi.org/10.5281/zenodo.10783820
Experimental models: Organisms/strains		
Mouse: PV^{Cre}: B6.129P2-Pvalb$^{tm1(cre)Arbr}$/J	The Jackson Laboratory	JAX: 008069
Mouse: Ai32: B6.129S-Gt(ROSA)26Sor$^{tm32(CAG—COP4*H134R/EYFP)Hze}$/J	The Jackson Laboratory	JAX: 012569
Mouse: SOM-IRES-Cre: Sst$^{tm2.1(cre)Zjh}$/J	The Jackson Laboratory	JAX: 013044
Mouse: Emx1-Cre: B6.129S2-Emx1$^{tm1(cre)Krj}$/J	The Jackson Laboratory	JAX: 005628
Software and algorithms		
MATLAB version 2019a	MathWorks	https://www.mathworks.com/help/matlab/release-notes-R2019a.html
BControl software	C. Brody, Princeton University	https://brodywiki.princeton.edu/bcontrol/index.php?title=Main_Page
StreamPix 8	Norpix	https://www.norpix.com/products/streampix/streampix.php
DeepLabCut	Mathis et al.[1]; Nath, Mathis et al.[2]	https://deeplabcut.github.io/DeepLabCut/docs/standardDeepLabCut_UserGuide.html
MClust	A.D. Redish	http://redishlab.neuroscience.umn.edu/MClust/MClust.html
Kilosort	Pachitariu et al.[3]	https://github.com/MouseLand/Kilosort
Original analysis code	This paper	Zenodo: https://doi.org/10.5281/zenodo.10783798
Other		
Piezo actuator	Piezo Systems	D220-A4-203YB
Piezo controller	Thorlabs	MDTC93B
LED	Thorlabs	M470F1
Optic fiber	Thorlabs	M43L01, TM200FL1B
Density filter	Thorlabs	NE530B
High speed CMOS camera	PhotonFocus	DR1-D1312-200-G2-8
Telecentric lens	Edmund Optics	Cat #: 55-349
Stereotaxic apparatus (Mouse Gas Anesthesia Head Holder)	David Kopf Instruments	Model 923-B

REAGENT or RESOURCE	SOURCE	IDENTIFIER
Silicon probe	Cambridge NeuroTech	ASSY-77 H3
Intan recording system	Intan Technologies	RHD2000
Laser, 473 nm	UltraLasers	DHOM-L-473-200mW
Acousto-optic modulator	QuantaTech	MTS110-A3-VIS